



Computed Tomography-Derived Normative Values of Right Ventricular Outflow Tract Structures in the Pediatric Population

Natalie Soszyn¹ · Justin Schweigert¹ · Salvador R. Franco¹ · Gareth J. Morgan¹ · Max Mitchell¹ · Jenny E. Zablah¹

Received: 26 September 2023 / Accepted: 16 February 2024

© The Author(s), under exclusive licence to Springer Science+Business Media, LLC, part of Springer Nature 2024

Abstract

Recent advances in available percutaneous device technology require accurate measurements and quantification of relationships between right ventricular outflow tract (RVOT) structures in children with and without congenital heart disease to determine device suitability. To date, no population study has described normal reference ranges of these measurements by computed tomography (CT). We aimed to establish normative values for four CT-derived measurements between RVOT structures from a heterogeneous population without heart disease and develop z scores useful for clinical practice. Patients without heart disease who underwent cardiac CT between April 2014 and February 2021 at Children's Hospital Colorado were included. Distance between the right ventricular (RV) apex to pulmonary valve (PV), PV to pulmonary trunk bifurcation, and bifurcation to the right and left pulmonary artery was measured. Previously validated models were used to normalize the measurements and calculate Z scores. Each measurement was plotted against BSA and Z scores distributions were used as reference lines. Three-hundred and sixty-four healthy patients with a mean age of 8.8 years (range 1–21), 58% male, and BSA of 1 m² (range 0.4–2.1) were analyzed. The Haycock formula was used to present data as predicted values for a given BSA and within equations relating each measurement to BSA. Predicted values and Z-score boundaries for all measurements are presented. We report CT-derived normative data for four measurements between RVOT structures from a heterogeneous cohort of healthy children. Knowledge of this normative data will be useful in both determining device fit and customizing future devices to accommodate the diverse pediatric size range.

Keywords Normative values · z scores · Right ventricular outflow tract

Abbreviations

BiVAD	Biventricular assist device
BSA	Body surface area
CT	Computed tomography
LPA	Left pulmonary artery
PT	Pulmonary trunk
PV	Pulmonary valve
RPA	Right pulmonary artery
RV	Right ventricle
RVOT	Right ventricular outflow tract
SD	Standard deviation
VAD	Ventricular assist device

Introduction

Normal diameters of right-sided cardiac structures in children have been well defined in the literature using echocardiographic, angiographic, and MRI data. [1–4] Defining lengths between these structures particularly using 3D cross-sectional imaging has not, however, been established. Accurate measurement of the distance between right ventricular outflow tract (RVOT) structures is vital for management of critically unwell children and young adults. Recent advances in advanced percutaneous technology require accurate measurements and quantification of relationships between RVOT structures to determine the patient selection and device suitability.

Pediatric mechanical circulatory support has advanced over the last decade with momentum building in the development and implantation of durable ventricular assist devices (VADs) in children. [5] Deterioration of right ventricular function is an acute event observed in a significant

✉ Jenny E. Zablah
jenny.zablah@childrenscolorado.org

¹ The Heart Institute, Children's Hospital Colorado, School of Medicine, University of Colorado Denver Anschutz Medical Campus, 13123 E 16th Ave, Aurora, CO 80045-2560, USA

proportion of patients after left ventricular assist device (LVAD) implantation, with approximately 25% of patients requiring biventricular assist device (BiVAD) support and is associated with higher adverse outcomes in the pediatric compared to the adult population. [5, 6] There is a burgeoning interest in developing devices specifically customized for the right ventricle to support a wide range of patient sizes, cardiac anatomy, and physiology.

Transcatheter pulmonary valve replacement (TPVR) has emerged as a minimally invasive approach to managing RVOT dysfunction due to significant pulmonary valve stenosis or regurgitation. [7–9] Pre-procedural imaging is imperative for identifying patient suitability and device sizing [10]. Similar to transcatheter aortic valve replacement, cross-sectional CT imaging has been shown to be a useful tool in procedural planning owing to the high isotropic spatial resolution, multiplanar reconstruction capability, and acquisition of volumetric data that can allow for 3D reconstruction and printed models useful for procedural guidance [11, 12]. The heterogeneity of patients referred for TPVR means that standardizing RVOT measurements to determine the appropriate valve or valve size has presented a challenge [11]. Knowledge of the relationship between the right ventricle, pulmonary valve, and branch pulmonary arteries is important in determining whether there is an appropriate landing zone for valve deployment.

The availability of a robust range of normal reference values can provide valuable information for current device selection and future development of customized devices for the RVOT tailored to accommodate the broad size, anatomic, and physiologic heterogeneity seen in the pediatric population. To date, no large population study has outlined normal reference ranges of these distance measurements by CT in healthy pediatric patients. We aimed to establish normative values for four CT-derived measurements between RVOT structures from a heterogeneous population with normal segmental anatomy and develop z scores useful for clinical practice.

Methods

Study Population

All patients who underwent a technically adequate cardiac CT completed between April 2014 and February 2021 at the Children's Hospital Colorado were considered for the study. Patients were selected if they had normal segmental anatomy. Demographic information including gender, ethnicity, and age at the time of the CT were collected retrospectively from electronic medical records. The Haycock formula was used in calculation of BSA for all subjects in the study. The study was approved by the Colorado Multi-Institutional Review Board (COMIRB #19-2292).

CT Image Acquisition and Data Analysis

All CT scans were single phase and non-gated. All CT scans were performed using our standardized institutional protocol. Non-gated CT angiography with single-phase reconstruction is used in our institution as it significantly reduces radiation dose without loss of image quality. Multiplanar Reconstruction (MPR) designed to standardize right ventricular measurements were rendered on a separate 3D workstation and measurements were retrospectively performed using a dedicated post-processing software (cvi42, Circle Cardiovascular Imaging, Calgary, Alberta, Canada) by a single operator. Distances between the apex of right ventricle (RV) to pulmonary valve (PV) (measure 1), PV to bifurcation of pulmonary trunk (measure 2), bifurcation of the pulmonary trunk to the first branch of the right pulmonary artery (RPA) (measure 3), and bifurcation of the pulmonary trunk to the first branch of the left pulmonary artery (LPA) (measure 4) were measured.

MPR was used to obtain the most appropriate plane for obtaining each measurement (Fig. 1). Measure 1 was first obtained using MPR from the sagittal plane which included

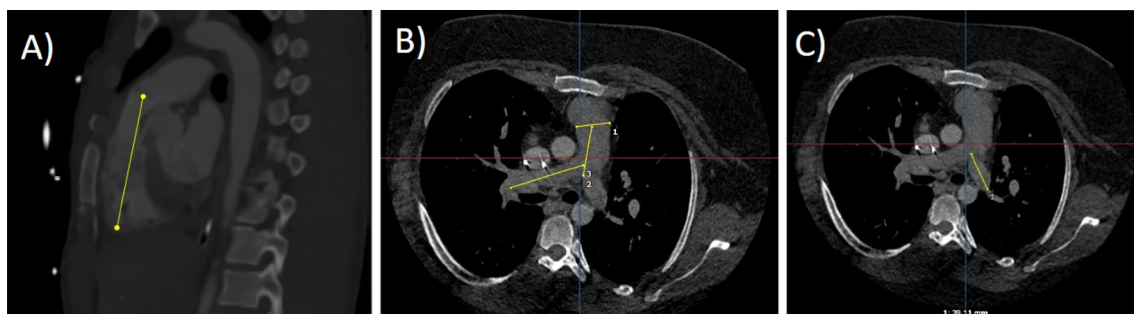


Fig. 1 Example of measurements. **A** Measure 1 (RV anterior apex to pulmonary valve) obtained in the sagittal plane. **B** Measure 2 (PV to PT bifurcation) and measure 3 (PT bifurcation to the first branch of

the RPA) obtained in the axial plane by first creating a horizontal line across the plane of the pulmonary valve. **C** Measure 4 (PT bifurcation to the first branch of the LPA) in the axial plane

the right ventricular apex and pulmonary valve annulus. Due to the variability of RV trabeculations between patients, measure 1 was obtained from the outer edge of the RV myocardium to standardize the measurement between patients. A second line was made perpendicular to the first line that bisected the PV. Using MPR to ensure the bifurcation of the pulmonary trunk and pulmonary valve annulus was simultaneously visualized in the same axial view, the distance from the pulmonary valve to the bifurcation of the pulmonary trunk (measure 2) was then obtained by drawing a line perpendicular from the line bisecting the PV to the pulmonary trunk bifurcation. Similarly, using MPR to ensure the length of the RPA could be visualized in the same plane, measure 3 was then obtained by measuring the distance from the PT bifurcation to the first branch of the RPA. Using a similar method, measure 4 was obtained from the bifurcation of the pulmonary trunk to the first branch of the LPA.

Statistical Methods

Statistical analysis was conducted using the statistical software package Stata v.15 (Statacorp LP, College Station, TX). Categorical data were expressed as frequency and percentage. Continuous data were presented as mean (range) if normally distributed and median (interquartile range) if not normally distributed. A Shapiro–Wilk test was performed to test the null hypothesis that there was no difference between the calculated and standard normal distribution of the continuous variables.

BSA was used as an independent variable in a regression analysis for the predicted mean value of each CT-derived measurement. Each measurement was plotted against BSA and then various non-linear models including logarithmic, exponential, polynomial, and quadratic models were evaluated to determine the “best fit” with tests for heteroscedasticity applied. A non-linear (polynomial) regression model using each observed measurement as the dependent variable (x) and BSA as the predictor (independent variable) was determined as the model of best fit.

Normalized data were then used to calculate z scores. To calculate a z -score, we defined the mean for each measurement and the corresponding standard deviation (SD). The z -score value conveys the magnitude of deviation from the mean. The z -score for each parameter can be calculated as follows:

$$Z = \frac{[(x/BSA) - \mu]}{\sigma}$$

where x is the observed measurement, μ is the mean of the standard population, and σ is the standard deviation of the sample population.

Standardized z scores are approximately normally distributed with mean = 0 and SD = 1. Therefore, $z = 0$ corresponds with the estimated mean and $z = \pm 1$ and ± 2 correspond to ± 1 and ± 2 SD from the estimated mean. In any normal distribution, 68% of the population is classified within its mean ± 1 SD and 95.4% within its mean ± 2 SD.

Results

Study Population

From a total of 378 who underwent cardiac CT during the defined period, data from 364 healthy children and young adults were included in the study. Fourteen were excluded due to inadequate CT image quality. Patient demographics can be seen in Table 1. The mean age of the study population was 8.8 years \pm 6.1 years (median 8 years, IQR 3–14 years), and there was 211 males and 153 females. Mean body weight was 32.5 \pm 22 kg (median 24.3 kg, IQR 14–48.1 kg), mean height was 123.5 \pm 34 cm (median 121.5 cm, IQR 94–155 cm), and mean BSA was 1.1 m² \pm 0.5 (median 1.0 m², IQR 0.6–1.5). Two-hundred and five patients (56%) were identified as being Caucasian, 92 (25%) Hispanic/Latino, 16 (5%) Black/African American, 9 (2%) Asian, 7 (2%) American Indian/Alaska Native, and 1 (2%) Native Hawaiian/Other Pacific Islander. Eighteen patients (4%) were identified as being more than one race and 16 (4%) did not specify any ethnicity.

Table 1 Patient demographics

	Total ($n = 364$)
Male: Female	211 (58%): 153 (42%)
Age (years)*	8 (3–14)
Weight (kg)*	24.3 (14–48.1)
Height (cm)*	121.5 (94–155)
BSA (m ²)*	1.0 (0.6–1.5)
Ethnicity/Race	
Caucasian	205 (56%)
Hispanic/Latino	92 (25%)
More than one Race	18 (5%)
Not specified	16 (4%)
Black/African American	16 (4%)
Asian	9 (2%)
American Indian/Alaska Native	7 (2%)
Native Hawaiian/Other Pacific Islander	1 (2%)

*Median (IQR)

Normal Distribution Curves

All four measurements were modeled against BSA. A non-linear (polynomial) regression model using BSA provided the best fit for all the data and satisfied the assumption of homoscedasticity and normality of residuals. The measurements plotted against BSA with four curves corresponding to z -score = 0, ± 1 , and ± 2 are displayed in Fig. 2. The superimposed solid line represents the estimated mean (labeled as $z=0$). The superimposed dotted lines represent $z = \pm 1$ and dashed lines $z = \pm 2$ above and below the mean line.

Calculation of Z Scores

Once the best fit relationship was defined, the mean and standard deviation were used at each BSA to determine the values for the corresponding z -score for each measurement, which is

presented in Table 2. The calculated mean and standard deviation for each measurement are provided in Table 3.

Z scores using our results can be calculated using two methods. The first is to use the graphs provided to find an approximate corresponding z -score for a given observed measurement and BSA. Secondly, Table 3 values can be used to calculate the z -score directly and more precisely. A z -score calculator is also provided for ease of calculation (Supplementary Material 1). For example, assuming the RV apex to pulmonary valve distance of 48.9 mm and the BSA of a patient is 1.0 m^2 , a z -score can be calculated with the mean of 67.96 mm and defined standard deviation of 9.52 mm as follows:

$$Z = \frac{[(48.9/1.0) - 67.96]}{9.52} = -2$$

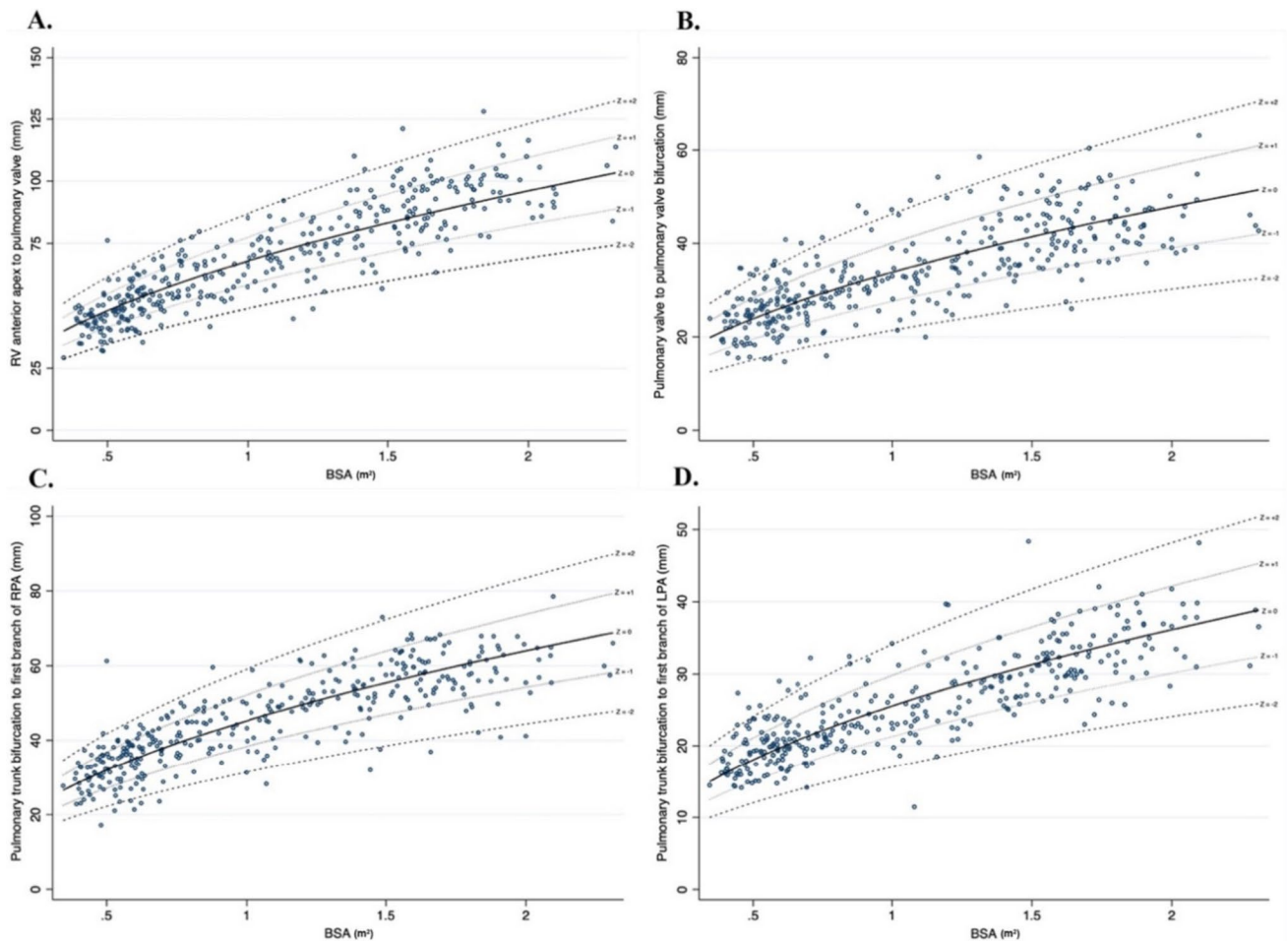


Fig. 2 Scatter plot of all four measurements compared to BSA with Z score as reference lines. Panels are separated by measurements as follows: **A** RV anterior apex to pulmonary valve; **B** pulmonary valve to bifurcation; **C** Pulmonary trunk bifurcation to RPA; **D** Pulmonary

trunk bifurcation to LPA. The solid middle line represents the mean ($Z=0$), the two outer dotted lines represent a Z score of ± 1 , and two outer dashed lines represent a Z score of ± 2

Table 2 Z-score to BSA for each CT-derived measurement

BSA (m ²)	RV anterior apex to PV			PV to PT bifurcation			PT bifurcation to RPA			PT bifurcation to LPA		
	Z score			Z score			Z score			Z score		
	-2	0	+2	-2	0	+2	-2	0	+2	-2	0	+2
0.5	34.6	48.1	61.5	15.1	23.9	32.8	22.2	32.0	41.8	12.0	18.1	24.1
0.6	37.9	52.6	67.4	16.6	26.2	35.9	24.3	35.1	45.8	13.2	19.8	26.4
0.7	40.9	56.9	72.8	17.9	28.3	38.8	26.3	37.9	49.4	14.3	21.4	28.5
0.8	43.8	60.8	77.8	19.1	30.3	41.4	28.1	40.5	52.9	15.2	22.9	30.5
0.9	46.4	64.5	82.5	20.3	32.1	43.9	29.8	42.9	56.1	16.2	24.2	32.3
1.0	48.9	68.0	87.0	21.4	33.8	46.3	31.4	45.3	59.1	17.0	25.6	34.1
1.1	51.3	71.3	91.2	22.4	35.5	48.6	33.0	47.5	62.0	17.9	26.8	35.7
1.2	53.6	74.4	95.3	23.4	37.1	50.7	34.4	49.6	64.7	18.7	28.0	28.0
1.3	55.8	77.5	99.2	24.4	38.6	52.8	35.8	51.6	67.4	19.4	29.1	29.1
1.4	57.9	80.4	103.0	25.3	40.0	54.8	37.2	53.5	69.9	20.2	30.2	40.3
1.5	59.9	83.2	106.5	26.2	41.5	56.7	38.5	55.4	72.4	20.9	31.3	41.7
1.6	61.9	86.0	110.0	27.0	42.8	58.6	39.8	57.2	74.7	21.5	32.3	43.1
1.7	63.8	88.6	113.4	27.9	44.1	60.4	41.0	59.0	77.0	22.2	33.3	44.4
1.8	65.6	91.2	116.7	28.7	45.4	62.1	42.2	60.7	79.3	22.9	34.3	45.7
1.9	67.4	93.7	119.9	29.5	46.6	63.8	43.3	62.4	81.4	23.5	35.2	47.0
2.0	69.2	96.1	123.0	30.2	47.9	65.5	44.4	64.0	83.6	24.1	36.1	48.2

RV right ventricle; PV pulmonary valve; PT pulmonary trunk; RPA right pulmonary artery; LPA left pulmonary artery

Table 3 Calculated mean and standard deviation for all CT-derived measurements

Measurement	Mean (μ)	Standard Deviation (σ)
RV anterior apex to pulmonary valve (mm)	67.96	9.52
PV to bifurcation of pulmonary trunk (mm)	33.84	6.23
PT bifurcation to first branch of the RPA (mm)	45.25	6.92
PT bifurcation to first branch of the LPA (mm)	25.55	4.26

Discussion

Normal diameters of right-sided cardiac structures including the right ventricle, pulmonary valve annulus, and branch pulmonary artery sizes in children have been well established in the past by echocardiographic, angiographic, and even MRI studies [1–4]. Information about the distance between the right ventricle, pulmonary valve, pulmonary artery bifurcation and branch pulmonary arteries in the pediatric population remains scarce. As there is increasing interest in implanting devices in the RVOT, knowledge about the normal range of distance between RVOT structures is important to aid in recognizing disease severity, in patient selection and pre-procedural planning, and in providing a benchmark for development of future

devices suitable for percutaneous placement in the RV in children and young adults. This is the first study to provide CT-derived, normalized values for four measurements between RVOT structures in a heterogeneous population of healthy children and young adults.

Patient selection for RVOT stents and TPVR depends on the identification of an appropriate site for implantation within the RVOT that will ensure device stability. The relative distances between the right ventricle, pulmonary valve, and branch pulmonary arteries are important in determining whether there is an appropriate landing zone for valve deployment. Cross-sectional CT imaging has been shown to be a useful tool in procedural planning owing to the high isotropic spatial resolution in all planes and cardiac phases [11, 13]. Shievano et al. highlighted the importance of 3D imaging in patient assessment and selection, and that the type of RVOT morphology in combination with RVOT size and distensibility allowed informed selection for currently available balloon-expandable valves [14]. Furthermore, there is additionally an increasing interest in using percutaneous VADs in the pediatric population as a less invasive alternative to extracorporeal membrane oxygenation (ECMO). Lasa et al. first reported the use of the Impella RP in combination with the Impella CP in a pediatric patient with acute severe biventricular failure and a multi-institutional experience was published in 2021 in adolescents as young as 14 years [15, 16]. Positioning is performed over a guidewire leaving the end of the device (pigtail configuration) at the MPA/LPA junction, with the exit port in the MPA and the inflow port

positioned in the inferior vena cava, near the right atrium [15, 16]. The device has a double-curved configuration that is ideally suited for the geometry of the right heart in adults and not necessarily for children. For this technology to be applicable to smaller pediatric patients, the device profile and configuration will need to be altered to conform to smaller hearts. Acknowledging this, our normative data provide a complementary tool that will aid in the expanded development of future similar devices for the wide size and anatomic variation seen in the pediatric population.

The use of BSA as expression of body size in children and the use of regression models to describe the relationship between body growth and the cardiovascular dimensions have been previously validated [3, 4, 17]. Similar to other studies, we identified a non-linear relationship between body growth and distances between RVOT structures. In the literature, there is limited description of the relationship between somatic growth and distance between RVOT structures. Our data show wider variability in all four measurements as BSA increases.

By establishing the ideal relationship between RVOT structures, the results of this study are likely of unique interest to pediatric cardiac surgeons and interventional cardiologists. In presenting normative data, we provide a reference point for physicians in describing disease severity, determining patient selection for procedures, and benchmarking the development of future devices. Further studies could also focus on the comparison between other imaging modalities to CT including echocardiographic and MRI data in establishing normative values for this population.

Strengths and Limitations

These data are derived from a homogeneous cohort of healthy children considering gender, age, and ethnic background. The study had a retrospective cohort design but had robust statistical methodology. Additionally, measurements were performed by a single operator minimizing interobserver variability and bias. The authors acknowledge that there is a degree of measurement and observational variance when comparing measurements between patients. However, by standardizing measurements to BSA, we expect measurement variance to be minimized. The power of this study may also be limited by the fact that only children with a BSA greater than 0.4 m^2 and less than 2.3 m^2 were included with a paucity of results greater than 2 m^2 . Even though a regression curve could be extrapolated from our data, we recommend caution for the use of our normative data for children at the extremes of BSA (i.e., less than 0.5 m^2 and greater than 2 m^2).

Another limitation that requires consideration that CT images were not ECG-gated. The first potential advantage of ECG-gating is that it minimizes and, in most cases,

eliminates cardiac motion artifact. Thus, cardiac measurements can be, in theory, more precise. ECG-gated scans generally have a longer acquisition time than comparable protocols without ECG-gating. Non-gated CT angiography with single-phase reconstruction significantly reduces radiation dose without loss of image quality. However, studies have shown that measurements in this setting obtained from non-gated CT images correlate with their ECG-gated counterparts as such image quality with non-gated CT was sufficient for the measurements obtained for this study [18].

Conclusion

We report CT-derived normative data for four measurements between cardio-pulmonary structures from a heterogeneous cohort of healthy children and young adults. These data may be useful in planning surgical or catheter-guided interventions in the management of children with congenital heart disease. Knowledge of this normative data will be useful in customizing future devices to accommodate the diverse size range, anatomy, and physiology of the pediatric population.

Clinical Perspective

Recent advances in advanced percutaneous technology require accurate measurements and quantification of relationships between RVOT structures to determine the patient selection and device suitability. The availability of a robust range of normal reference values can provide valuable information for current device selection and future development of customized devices for the RVOT tailored to accommodate the broad size, anatomic, and physiologic heterogeneity seen in the pediatric population. We report CT-derived normative data for four measurements between cardio-pulmonary structures from a heterogeneous cohort of healthy children and young adults. These data may be useful in planning surgical or catheter-guided interventions in the management of children with congenital heart disease.

Supplementary Information The online version contains supplementary material available at <https://doi.org/10.1007/s00246-024-03456-2>.

Acknowledgements None.

Author contributions JZ, MM and GM conceived the idea of developing normative values between RVOT structures. JS was responsible for data collection. NS and SR conducted the data analysis. NS wrote the manuscript in discussion with JZ. GM and JZ revised the manuscript for quality. All authors contributed to the article and approved the submitted version.

Declarations

Competing interest The authors have no relevant financial or non-financial interests to disclose.

Ethical Approval This retrospective chart review study involving human participants was in accordance with the ethical standards of the institutional and national research committee and with the 1964 Helsinki Declaration and its later amendments or comparable ethical standards. The Human Investigation Committee (IRB) of the Children's Hospital Colorado approved this study.

References

- Knobel Z, Kellenberger CJ, Kaiser T, Albisetti M, Bergsträsser E, Valsangiacomo Buechel ER (2011) Geometry and dimensions of the pulmonary artery bifurcation in children and adolescents: assessment in vivo by contrast-enhanced MR-angiography. *Int J Cardiovasc Imaging* 27(3):385–396
- Gutgesell HP, French M (1991) Echocardiographic determination of aortic and pulmonary valve areas in subjects with normal hearts. *Am J Cardiol* 68(8):773–776
- Pettersen MD, Du W, Skeens ME, Humes RA (2008) Regression equations for calculation of z scores of cardiac structures in a large cohort of healthy infants, children, and adolescents: an echocardiographic study. *J Am Soc Echocardiogr* 21(8):922–934
- Snider AR, Enderlein MA, Teitel DF, Juster RP (1984) Two-dimensional echocardiographic determination of aortic and pulmonary artery sizes from infancy to adulthood in normal subjects. *Am J Cardiol* 53(1):218–224
- VanderPluym CJ, Fynn-Thompson F, Blume ED (2014) Ventricular assist devices in children. *Circulation* 129(14):1530–1537
- Baez Hernandez N, Kirk R, Sutcliffe D, Davies R, Jaquiss R, Gao A et al (2020) Utilization and outcomes in biventricular assist device support in pediatrics. *J Thorac Cardiovasc Surg* 160(5):1301–8.e2
- Morgan GJ, Sadeghi S, Salem MM, Wilson N, Kay J, Rothman A et al (2019) SAPIEN valve for percutaneous transcatheter pulmonary valve replacement without “pre-stenting”: a multi-institutional experience. *Catheter Cardiovasc Interv* 93(2):324–329
- Alkashkari W, Albugami S, Abbad M, Niyazi A, Alsubei A, Hijazi ZM (2020) Transcatheter pulmonary valve replacement in pediatric patients. *Expert Rev Med Devices* 17(6):541–554
- Holzer RJ, Hijazi ZM (2016) Transcatheter pulmonary valve replacement: State of the art. *Catheter Cardiovasc Interv* 87(1):117–128
- Chung R, Taylor AM (2014) Imaging for preintervention planning: transcatheter pulmonary valve therapy. *Circ Cardiovasc Imaging* 7(1):182–189
- Curran L, Agrawal H, Kallianos K, Kheiwa A, Lin S, Ordovas K et al (2020) Computed tomography guided sizing for transcatheter pulmonary valve replacement. *Int J Cardiol Heart Vasc* 29:100523
- Revels JW, Wang SS, Gharai LR, Febbo J, Fadl S, Bastawrous S (2021) The role of CT in planning percutaneous structural heart interventions: Where to measure and why. *Clin Imaging* 76:247–264
- Sun X, Hao Y, Sebastian Kiekenap JF, Emeis J, Steitz M, Breitenstein-Attach A et al (2022) Four-dimensional computed tomography-guided valve sizing for transcatheter pulmonary valve replacement. *J Vis Exp*. <https://doi.org/10.3791/63367>
- Schievano S, Coats L, Migliavacca F, Norman W, Frigiola A, Deanfield J et al (2007) Variations in right ventricular outflow tract morphology following repair of congenital heart disease: implications for percutaneous pulmonary valve implantation. *J Cardiovasc Magn Reson* 9(4):687–695
- Lasa JJ, Castellanos DA, Denfield SW, Dreyer WJ, Tume SC, Justino H et al (2018) First report of biventricular percutaneous impella ventricular assist device use in pediatric patients. *Asaio J* 64(5):e134–e137
- Qureshi AM, Turner ME, O'Neill W, Denfield SW, Aghili N, Badiye A et al (2020) Percutaneous Impella RP use for refractory right heart failure in adolescents and young adults—a multicenter US experience. *Catheter Cardiovasc Interv* 96(2):376–81
- Zilberman MV, Khoury PR, Kimball RT (2005) Two-dimensional echocardiographic valve measurements in healthy children: gender-specific differences. *Pediatr Cardiol* 26(4):356–360
- Lu MT, Cai T, Ersoy H, Whitmore AG, Levit NA, Goldhaber SZ, Rybicki FJ (2009) Comparison of ECG-gated versus non-gated CT ventricular measurements in thirty patients with acute pulmonary embolism. *Int J Cardiovasc Imaging* 25(1):101–107. <https://doi.org/10.1007/s10554-008-9342-0>

Publisher's Note Springer Nature remains neutral with regard to jurisdictional claims in published maps and institutional affiliations.

Springer Nature or its licensor (e.g. a society or other partner) holds exclusive rights to this article under a publishing agreement with the author(s) or other rightsholder(s); author self-archiving of the accepted manuscript version of this article is solely governed by the terms of such publishing agreement and applicable law.